Shrinkage Stresses in a Thick-Walled Viscoelastic Cylinder Bonded to a Rigid Case†

A. M. FREUDENTHAL*
Columbia University

M. SHINOZUKA**
Columbia University

Summary

Stresses and strains in a thick-walled cylinder of viscoelastic material of infinite length due to homogeneous shrinkage of the material are discussed. Two models, one of which assumes a standard solid response in shear and elastic response under volumetric strain, the other standard solid response for both conditions, are employed in order to demonstrate the effect of volume viscosity. Two different (initial) Poisson's ratios are considered to find the effect of the elastic compressibility of the viscoelastic material. The expression for the first invariant of the stress tensor is given and a measure of triaxiality is computed because of their assumed sensitivity with respect to crack initiation in viscoelastic materials.

Symbols

a,b	= inner and outer radius of thick-walled cylinder
e_{ij}	= components of strain deviation tensor
E	= Young's modulus
$\bar{E}(p)$	= a function of p which replaces E in elastic solutions to produce transformed viscoelastic solutions
G,G_1,G_2	= shear moduli
$H(t)$	= unit step function
J_1	= σ_{kk}, the first invariant of stress tensor
J_2'	= the second invariant of stress deviation tensor
K,K_1,K_2	= bulk moduli
p	= transform parameter in the Laplace transformation
P,Q,P',Q'	= differential operators with respect to time
$\bar{P}(p),\bar{Q}(p),\bar{P}'(p),\bar{Q}'(p)$	= polynomials in p
r,θ,z	= cylindrical coordinates
s_{ij}	= components of stress deviation tensor
t	= time
u	= radial displacement
α	= coefficient of linear thermal expansion
ΔT	= temperature variation
$3\epsilon',3\epsilon_0',3\epsilon_1'$	= volumetric deformations due to imposed shrinkage
$\bar{\epsilon}'(p)$	= the Laplace transform of ϵ'
ϵ_{ij}	= components of strain tensor
ϵ_{kk}	= sum of normal components of strain tensor
$\epsilon_r,\epsilon_\theta,\epsilon_z$	= radial, tangential, and axial strain
$\bar{\epsilon}_r(p),\bar{\epsilon}_\theta(p),\bar{\epsilon}_z(p)$	= transformed radial, tangential, and axial strain
η_2	= coefficient of shear viscosity
κ_2	= coefficient of volume viscosity
ν,ν_0	= Poisson ratios
$\bar{\nu}(p)$	= a function of p which replaces ν in elastic solutions to produce transformed viscoelastic solutions
ρ	= b/a
σ_{ij}	= components of stress tensor
σ_{kk}	= sum of normal components of stress tensor
$\sigma_r,\sigma_\theta,\sigma_z$	= radial, tangential, and axial stress
$\bar{\sigma}_r(p),\bar{\sigma}_\theta(p),\bar{\sigma}_z(p)$	= transformed radial, tangential, and axial stress
τ_0	= time parameter
τ_2,τ_2'	= shear and bulk relaxation time
ϕ	= stress function

Received by IAS March 12, 1962. Revised and received October 3, 1962.

† This research was supported by the Office of Naval Research under Contract Nonr 266(78).

*Professor of Civil Engineering.

** Assistant Professor of Civil Engineering.

(1) Introduction

IN CYLINDRICAL SOLID PROPELLANT GRAINS, separation of propellant and casing or cracks within the propellant formed during storage are assumed to be due mainly to shrinkage of the propellant material. The fact that the response of the material is viscoelastic rather than elastic reduces the severity of the shrinkage stresses to some extent, but does not relieve them entirely, since the stress-relaxation characteristic of real viscoelastic materials only involves the deviatoric components of the stresses, unless there is a significant volume-viscosity present. The assumed viscoelastic response in shear (standard solid) represents the simplest physical approximation to the behavior of an elastomer, since it shows the characteristic form of the frequency (or temperature) dependence of the shear modulus, although the primary transition of the model is much steeper than that of real elastomers. The alternative assumptions concerning the volumetric response are designed to illustrate the effect of volume-viscosity.

The purpose of the present investigation is to find stresses and strains in a thick-walled viscoelastic cylinder due to homogeneous shrinkage and particularly to establish the intensity of the tangential stresses in the cylinder close to the interface of case and cylinder, as well as the radial stresses acting on the interface, for specific assumption concerning the viscoelastic response of the propellant materials that are qualitatively consistent with their observed behavior. In view of the crack-sensitivity of viscoelastic materials under bi- and triaxial tensile stress, it seemed important to investigate the degree of triaxiality of the cylinder stresses and in particular the effect of stress-relaxation on the triaxial states of tension developing in the vicinity of the interface.

Since the shrinkage is assumed to be homogeneous

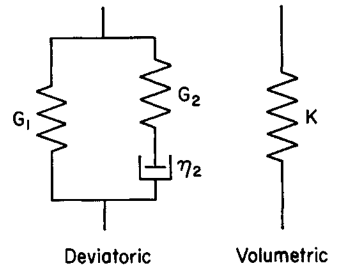

FIG. 1. Model I of the mechanical response of the material.

throughout the cylinder, the volumetric deformation $3\epsilon'$ is a function of time, not of space, as long as the cylinder is free from boundary constraints. The dependence of ϵ' on time t is assumed to be described by the function

$$\epsilon' = [\epsilon_0' + \epsilon_1'(1 - e^{-t/\tau_0})]H(t) \tag{1}$$

where ϵ_0' and ϵ_1' are constants and $H(t)$ is the unit step function. It should be noted that ϵ' is negative for shrinkage since the usual convention of ϵ' to be positive for expansion is adopted here according to the theory of elasticity.

The analysis produces a rigorous solution of the physical problem when shrinkage is spontaneous being due to chemical reactions and therefore homogeneous throughout the cylinder, while it is an approximation if the shrinkage is caused by the decrease of the ambient temperature (from curing to storage temperature in case of solid propellant) since then the nonuniform distribution of temperature in space not only produces nonhomogeneous shrinkage but also alters the material properties. The stress analysis due to nonhomogeneous shrinkage imposed on nonhomogeneous viscoelastic materials would be considerably lengthy and is a problem for future study.

The cylinder is considered to be of infinite length so as to reduce the analysis to the case of plane strain. Furthermore, it is assumed that the cylinder is contained in a rigid case; thus the tangential and radial components of the displacement at the outer surface are zero, while the inner surface is traction free. The assumption of a rigid case is not only expedient but it also produces the severest shrinkage stresses.

(2) Models of the Material

Two models for the viscoelastic material are considered. Model 1 combines deviatoric and volumetric stress-strain relations represented respectively by a standard solid and an elastic medium (Fig. 1). When s_{ij} and e_{ij} denote components of deviatoric stress and strain and σ_{kk} and ϵ_{kk} sums of the normal components of stress and strain, these relations are[1]

$$\left.\begin{aligned} \mathbf{P}s_{ij} &= \mathbf{Q}e_{ij} \\ \mathbf{P} &= \partial/\partial t + 1/\tau_2 \\ \mathbf{Q} &= 2G\partial/\partial t + 2G_1/\tau_2 \\ \mathbf{P}'\sigma_{kk} &= \mathbf{Q}'\epsilon_{kk} \\ \mathbf{P}' &= 1, \mathbf{Q}' = 3K \end{aligned}\right\} \tag{2}$$

where G_1, G_2, K are elastic constants, η_2 is the coefficient of viscosity in shear as shown in Fig. 1, $\tau_2 = \eta_2/G_2$ the relaxation-time and $G = G_1 + G_2$ the unrelaxed shear modulus.

In Model 2 both deviatoric and volumetric stress-strain relations are represented by standard solids (Fig. 2)[1]

$$\left.\begin{aligned} \mathbf{P}s_{ij} &= \mathbf{Q}e_{ij} \\ \mathbf{P} &= \partial/\partial t + 1/\tau_2 \\ \mathbf{Q} &= 2G\partial/\partial t + 2G_1/\tau_2 \\ \mathbf{P}'\sigma_{kk} &= \mathbf{Q}\epsilon_{kk} \\ \mathbf{P}' &= \partial/\partial t + 1/\tau_2' \\ \mathbf{Q} &= 3K\partial/\partial t + 3K_1/\tau_2' \end{aligned}\right\} \tag{3}$$

where G_1, G_2, K_1, K_2 are elastic constants, η_2, κ_2 are the coefficients of shear and bulk viscosity as shown in Fig. 2, $\tau_2' = \kappa_2/K_2$ the bulk relaxation time and $K = K_1 + K_2$ the unrelaxed bulk modulus.

The Laplace transform of Eqs. (1), (2), and (3) with respect to time under initially zero condition produces Eqs. (4)–(6) respectively.

$$\bar{\epsilon}'(p) = [\epsilon_0'p + (\epsilon_0' + \epsilon_1')/\tau_0]/p(p + 1/\tau_0) \tag{4}$$

$$\left.\begin{aligned} \bar{\mathbf{P}}(p)\bar{s}_{ij}(p) &= \bar{\mathbf{Q}}(p)\bar{e}_{ij}(p) \\ \bar{\mathbf{P}}(p) &= p + 1/\tau_2, \\ \bar{\mathbf{Q}}(p) &= 2Gp + 2G_1/\tau_2 \\ \bar{\mathbf{P}}'(p)\bar{\sigma}_{kk}(p) &= \bar{\mathbf{Q}}'(p)\bar{\epsilon}_{kk}(p) \\ \bar{\mathbf{P}}'(p) &= 1, \ \bar{\mathbf{Q}}'(p) = 3K \end{aligned}\right\} \tag{5}$$

$$\left.\begin{aligned} \bar{\mathbf{P}}(p)\bar{s}_{ij}(p) &= \bar{\mathbf{Q}}(p)\bar{e}_{ij}(p) \\ \bar{\mathbf{P}}(p) &= p + 1/\tau_2, \\ \bar{\mathbf{Q}}(p) &= 2Gp + 2G_1/\tau_2 \\ \bar{\mathbf{P}}'(p)\bar{\sigma}_{kk}(p) &= \bar{\mathbf{Q}}'(p)\bar{\epsilon}_{kk}(p) \\ \bar{\mathbf{P}}'(p) &= p + 1/\tau_2', \\ \bar{\mathbf{Q}}'(p) &= 3Kp + 3K_1/\tau_2' \end{aligned}\right\} \tag{6}$$

where p is the transform parameter.

The replacement of ϵ' by $\bar{\epsilon}'(p)$ as well as the elastic constants E and ν by the viscoelastic operators $\bar{\mathbf{E}}(p)$ and $\bar{\nu}(p)$ in the associated elastic solution gives, by virtue of the elastic-viscoelastic analogy,[1] the transformed solution which in turn produces upon inversion the viscoelastic solution, where $\bar{\mathbf{E}}(p)$ and $\bar{\nu}(p)$ are

$$\left.\begin{aligned} \bar{\mathbf{E}}(p) &= \frac{3\bar{\mathbf{Q}}'(p)\bar{\mathbf{Q}}(p)}{2\bar{\mathbf{Q}}'(p)\bar{\mathbf{P}}(p) + \bar{\mathbf{Q}}(p)\bar{\mathbf{P}}'(p)} \\ \bar{\nu}(p) &= \frac{\bar{\mathbf{Q}}'(p)\bar{\mathbf{P}}(p) - \bar{\mathbf{Q}}(p)\bar{\mathbf{P}}'(p)}{2\bar{\mathbf{Q}}'(p)\bar{\mathbf{P}}(p) + \bar{\mathbf{Q}}(p)\bar{\mathbf{P}}'(p)} \end{aligned}\right\} \tag{7}$$

(3) Elastic Solution

The associated elastic problem is to find stresses and strains in a hollow cylinder of infinite length subject to uniform volume change that might also be associated with a uniform temperature change ΔT under the specified boundary condition. The equation of equilibrium in cylindrical coordinates is

$$(d\sigma_r/dr) + [(\sigma_r - \sigma_\theta)/r] = 0$$

where σ_r and σ_θ are radial and tangential stresses.

From the strain-deformation relations

$$\epsilon r = du/dr \quad \text{and} \quad \epsilon_\theta = u/r$$

the compatibility equation

$$r(d\epsilon_\theta/dr) + \epsilon_\theta - \epsilon_r = 0$$

is obtained where ϵ_r and ϵ_θ are the radial and tangential strain components, the radial displacement u being a function of r alone.

The stress-strain relations are

$$\epsilon_r = \frac{1+\nu}{E}[(1-\nu)\sigma_r - \nu\sigma_\theta] + (1+\nu)\epsilon'$$

$$\epsilon_\theta = \frac{1+\nu}{E}[(1-\nu)\sigma_\theta - \nu\sigma_\theta] + (1+\nu)\epsilon'$$

$$\epsilon_z = 0$$

where ϵ' might be considered as $\epsilon' = \alpha\Delta T$ where α represents the coefficient of linear thermal expansion and ΔT is a temperature variation being negative for shrinkage.

The introduction of a stress function ϕ such that

$$\sigma_r = \phi/r,\ \sigma_\theta = d\phi/dr$$

produces the compatibility equation in terms of ϕ

$$\frac{d^2\phi}{dr^2} + \frac{1}{r}\cdot\frac{d\phi}{dr} - \frac{\phi}{r^2} = -\frac{E}{1-\nu}\cdot\frac{d\epsilon'}{dr}$$

The solution of the above equation, with the boundary condition $u = 0$ at $r = b$ and $\sigma_r = 0$ at $r = a$ under the assumption $d\epsilon'/dr = 0$, is

$$\phi = -\frac{E\rho^2\epsilon'}{1+(1-2\nu)\rho^2}(r - a^2/r)$$

where a and b denote the inner and outer radius of the hollow cylinder and the radius ratio $b/a = \rho$.

Therefore, the associated stress and strain components are

$$\left.\begin{aligned}\sigma_r &= -\rho^2(1 - a^2/r^2)\\ \sigma_\theta &= -\rho^2(1 + a^2/r^2)\\ \sigma_z &= -(1+\rho^2)\end{aligned}\right\} \times \frac{E\epsilon'}{1+(1-2\nu)\rho^2} \tag{8}$$

$$\left.\begin{aligned}\epsilon_r &= (1 + \rho^2a^2/r^2)\\ \epsilon_\theta &= (1 - \rho^2a^2/r^2)\\ \epsilon_z &= 0\end{aligned}\right\} \times \frac{(1+\nu)\epsilon'}{1+(1-2\nu)\rho^2} \tag{9}$$

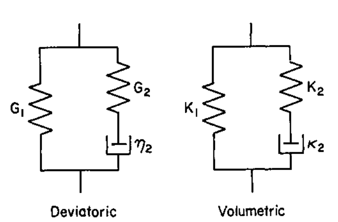

FIG. 2. Model II of the mechanical response of the material.

(4) Viscoelastic Stress and Strain Components

The replacement of ϵ', E, and ν in Eqs. (8) and (9) respectively by $\bar{\epsilon}'$ and the associated viscoelastic operators $\bar{E}(p)$ and $\bar{\nu}(p)$ indicated in Eqs. (4) and (7) produces the transformed stresses and strains given below;

(a) Model I

$$\left.\begin{aligned}\bar{\sigma}_r(p) &= -\frac{9\rho^2(1 - a^2/r^2)}{3K + (1+3\rho^2)G}\bar{F}\sigma(p)\\ \bar{\sigma}_\theta(p) &= -\frac{9\rho^2(1 + a^2/r^2)}{3K + (1+3\rho^2)G}\bar{F}\sigma(p)\\ \bar{\sigma}_z(p) &= -\frac{9(1+\rho^2)}{3K + (1+3\rho^2)G}\bar{F}\sigma(p)\\ \bar{F}\sigma(p) &= -\\ &\frac{[\epsilon_0'p + (\epsilon_0' + \epsilon_1')/\tau_0]K(Gp + G_1/\tau_2)}{p(p + 1/\tau_0)(p - k)}\end{aligned}\right\} \tag{10}$$

$$\left.\begin{aligned}\bar{\epsilon}_r(p) &= \frac{9(1 + \rho^2a^2/r^2)}{2[3K + (1+3\rho^2)G]}\bar{F}\epsilon(p)\\ \bar{\epsilon}_\theta(p) &= \frac{9(1 - \rho^2a^2/r^2)}{2[3K + (1+3\rho^2)G]}\bar{F}\epsilon(p)\\ \bar{F}\epsilon(p) &= \frac{[\epsilon_0'p + (\epsilon_0' + \epsilon_1')/\tau_0]K(p + 1/\tau_2)}{p(p + 1/\tau_0)(p - k)}\end{aligned}\right\} \tag{11}$$

where

$$k = -\frac{3K + (1+3\rho^2)G_1}{3K + (1+3\rho^2)G}\cdot\frac{1}{\tau_2} \tag{12}$$

The inverse transform of Eqs. (10) and (11) produces

$$\left.\begin{aligned}\sigma_r(t) &= -\frac{9\rho^2(1 - a^2/r^2)}{3K + (1+3\rho^2)G}F_\sigma(t)\\ \sigma_\theta(t) &= -\frac{9\rho^2(1 + a^2/r^2)}{3K + (1+3\rho^2)G}F_\sigma(t)\\ \sigma_z(t) &= -\frac{9(1+\rho^2)}{3K + (1+3\rho^2)G}F_\sigma(t)\\ F_\sigma(t) &= A + Be^{-t/\tau_0} + Ce^{kt}\end{aligned}\right\} \tag{13}$$

where

$$A = -(\epsilon_0' + \epsilon_1')G_1K/k\tau_2$$

$$B = \epsilon_1'(G_1/\tau_2 - G/\tau_0)K/(k + 1/\tau_0)$$

$$C = [\epsilon_0'k + (\epsilon_0' + \epsilon_1')/\tau_0] \times (Gk + G_1/\tau_2)K/k(k + 1/\tau_0)$$

as well as

$$\left.\begin{aligned}\epsilon_r(t) &= \frac{9(1 + \rho^2a^2/r^2)}{2[3K + (1+3\rho^2)G]}F_\epsilon(t)\\ \epsilon_\theta(t) &= \frac{9(1 - \rho^2a^2/r^2)}{2[3K + (1+3\rho^2)G]}F_\epsilon(t)\\ F_\epsilon(t) &= A' + B'e^{-t/\tau_0} + C'e^{kt}\end{aligned}\right\} \tag{14}$$

where

$$A' = -(\epsilon_0' + \epsilon_1')K/k\tau_2$$
$$B' = \epsilon_1'(1/\tau_2 - 1/\tau_0)K/(k + 1/\tau_0)$$
$$C' = [\epsilon_0'k + (\epsilon_0' + \epsilon_1')/\tau_0] \times (k + 1/\tau_2)K/k(k + 1/\tau_0)$$

(b) Model 2

$$\left.\begin{aligned} \bar\sigma_r(p) &= -\frac{9\rho^2(1 - a^2/r^2)}{3K + (1 + 3\rho^2)G}\bar F_\sigma(p) \\ \bar\sigma_\theta(p) &= -\frac{9\rho^2(1 + a^2/r^2)}{3K + (1 + 3\rho^2)G}\bar F_\sigma(p) \\ \bar\sigma_z(p) &= -\frac{9(1 + \rho^2)}{3K + (1 + 3\rho^2)G}\bar F_\sigma(p) \\ \bar F_\sigma(p) &= \frac{[\epsilon_0'p + (\epsilon_0' + \epsilon_1')/\tau_0] \times (Gp + G_1/\tau_2)(Kp + K_1/\tau_2')}{p(p + 1/\tau_0)(p - k_1)(p - k_2)} \end{aligned}\right\} \quad (15)$$

as well as

Model	ν_0	Volumetric Deformation $3\epsilon'$	Designation
I	0.3	Eq. (20)	I(1)
I	0.3	Eq. (21)	I(2)
II	0.3	Eq. (20)	II(1)
II	0.3	Eq. (21)	II(2)
I	0.49	Eq. (20)	I'(1)
I	0.49	Eq. (21)	I'(2)

TABLE 1.

$$\left.\begin{aligned} \bar\epsilon_r(p) &= \frac{9(1 + \rho^2a^2/r^2)}{2[3K + (1 + 3\rho^2)G]}\bar F_\epsilon(p) \\ \bar\epsilon_\theta(p) &= \frac{9(1 - \rho^2a^2/r^2)}{2[3K + (1 + 3\rho^2)G]}\bar F_\epsilon(p) \\ \bar F_\epsilon(p) &= \frac{[\epsilon_0'p + (\epsilon_0' + \epsilon_1')/\tau_0] \times (p_1 + 1/\tau_2)(Kp + K_1/\tau_2')}{p(p + 1/\tau_0)(p - k_1)(p - k_2)} \end{aligned}\right\} \quad (16)$$

and

$$\left.\begin{matrix} k_1 \\ k_2 \end{matrix}\right\} = -\frac{3(K_1/\tau_2' + K/\tau_2) + (1 + 3\rho^2)(G_1/\tau_2 + G/\tau_2')}{2[3K + (1 + 3\rho^2)G]} \pm \sqrt{\frac{[3(K_1/\tau_2' + K/\tau_2) + (1 + 3\rho^2)(G_1/\tau_2 + G/\tau_2')]^2}{4[3K + (1 + 3\rho^2)G]^2} - \frac{3K_1 + (1 + 3\rho^2)G_1}{[3K + (1 + 3\rho^2)G]\tau_2\tau_2'}} \quad (17)$$

The inverse transform of Eqs. (15) and (16) gives

$$\left.\begin{aligned} \sigma_r(t) &= -\frac{9\rho^2(1 - a^2/r^2)}{3K + (1 + 3\rho^2)G}F_\sigma(t) \\ \sigma_\theta(t) &= -\frac{9\rho^2(1 + a^2/r^2)}{3K + (1 + 3\rho^2)G}F_\sigma(t) \\ \sigma_z(t) &= -\frac{9(1 + \rho^2)}{3K + (1 + 3\rho^2)G}F_\sigma(t) \\ F_\sigma(t) &= A + Be^{-t/\tau_0} + Ce^{k_1t} + De^{k_2t} \end{aligned}\right\} \quad (18)$$

where

$$A = K_1G_1(\epsilon_0' + \epsilon_1')/k_1k_2\tau_2\tau_2'$$
$$B = -\epsilon_1'(G_1/\tau_2 - G/\tau_0)(K_1/\tau_2' - K/\tau_0) \div (k_1 + 1/\tau_0)(k_2 + 1/\tau_0)$$
$$C = [\epsilon_0'k_1 + (\epsilon_0' + \epsilon_1')/\tau_0](Gk_1 + G_1/\tau_2) \times (Kk_1 + K_1/\tau_2')/k_1(k_1 + 1/\tau_0)(k_1 - k_2)$$
$$D = -[\epsilon_0'k_2 + (\epsilon_0' + \epsilon_1')/\tau_0](Gk_2 + G_1/\tau_2) \times (Kk_2 + K_1/\tau_2')/k_2(k_2 + 1/\tau_0)(k_1 - k_2)$$

as well as

$$\left.\begin{aligned} \epsilon_r(t) &= \frac{9(1 + \rho^2a^2/r^2)}{2[3K + (1 + 3\rho^2)G]}F_\epsilon(t) \\ \epsilon_\theta(t) &= \frac{9(1 - \rho^2a^2/r^2)}{2[3K + (1 + 3\rho^2)G]}F_\epsilon(t) \\ F_\epsilon(t) &= A' + B'e^{-t/\tau_0} + C'e^{k_1t} + D'e^{k_2t} \end{aligned}\right\} \quad (19)$$

where

$$A' = K_1(\epsilon_0' + \epsilon_1')/k_1k_2\tau_2\tau_2'$$
$$B' = -\epsilon_1'(1/\tau_2 - 1/\tau_0)(K_1/\tau_2' - K/\tau_0) \div (k_1 + 1/\tau_0)(k_2 + 1/\tau_0)$$
$$C' = [\epsilon_0'k_1 + (\epsilon_0' + \epsilon_1')/\tau_0](k_1 + 1/\tau_2) \times (Kk_1 + K_1/\tau_2')/k_1(k_1 + 1/\tau_0)(k_1 - k_2)$$
$$D' = -[\epsilon_0'k_2 + (\epsilon_0' + \epsilon_1')/\tau_0](k_2 + 1/\tau_2) \times (Kk_2 + K_1/\tau_2')/k_2(k_2 + 1/\tau_0)(k_1 - k_2)$$

The above results will be illustrated by numerical examples.

(5) Numerical Example (a)

In the elastic medium Poisson's ratio ν_0 is related to G and K by $G/K = 1.5\,(1 - 2\nu_0)/(1 + \nu_0)$.

For the numerical examples, the assumption is made that (*a*) $\nu_0 = 0.3$ ($G/K = 0.461538$) and $G_1/G_2 = 0.1$ for Model I, (*b*) $\nu_0 = 0.49$ ($G/K = 0.0201342$) and $G_1/G_2 = 0.1$ for Model I, (*c*) $\nu_0 = 0.3$ ($G/K = 0.461538$), $G_1/G_2 = 0.1$, $K_1 = K_2 = K/2$, and $\tau_2' = \tau_2$ for Model II. Furthermore, two types of volumetric deformations are assumed

$$\epsilon' = \epsilon_0'H(t) \quad (20)$$

$$\epsilon' = \epsilon_1'(1 - e^{-t/\tau_2})H(t) \quad (21)$$

Since Eq. (20) is a limit of Eq. (1) when τ_0 approaches infinity and Eq. (21) is the result of the substitution of $\epsilon_0' = 0$ and $\tau_0 = \tau_2$ into Eq. (1), the function $\bar F_\sigma(p)$ and

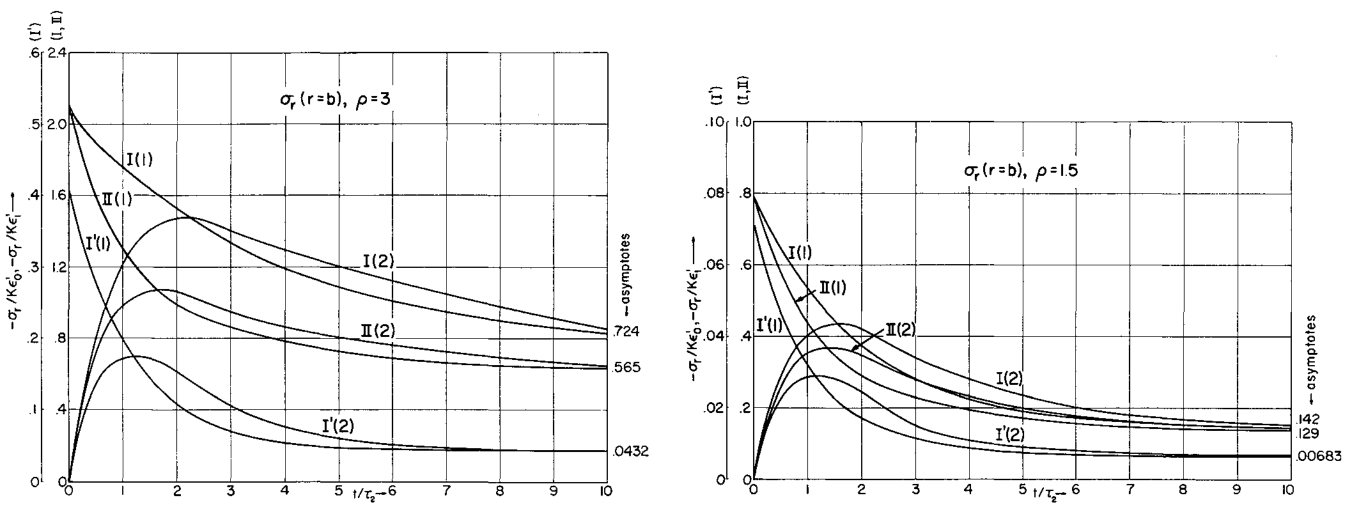

FIG. 3. Radial stress σ_r at $r = b$ as a function of time (t/τ_2).

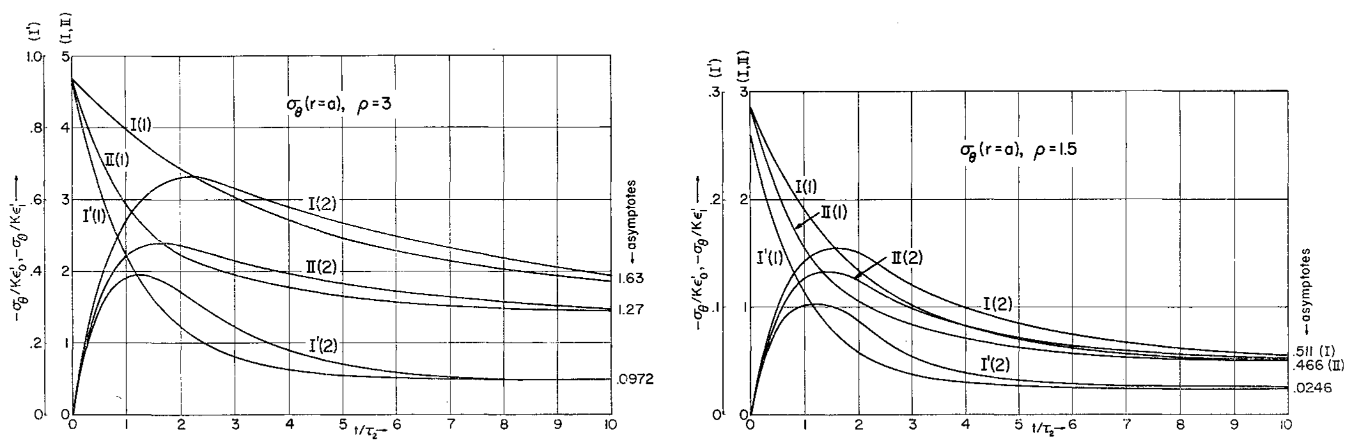

FIG. 4. Tangential stress σ_θ at $r = a$ as a function of time (t/τ_2).

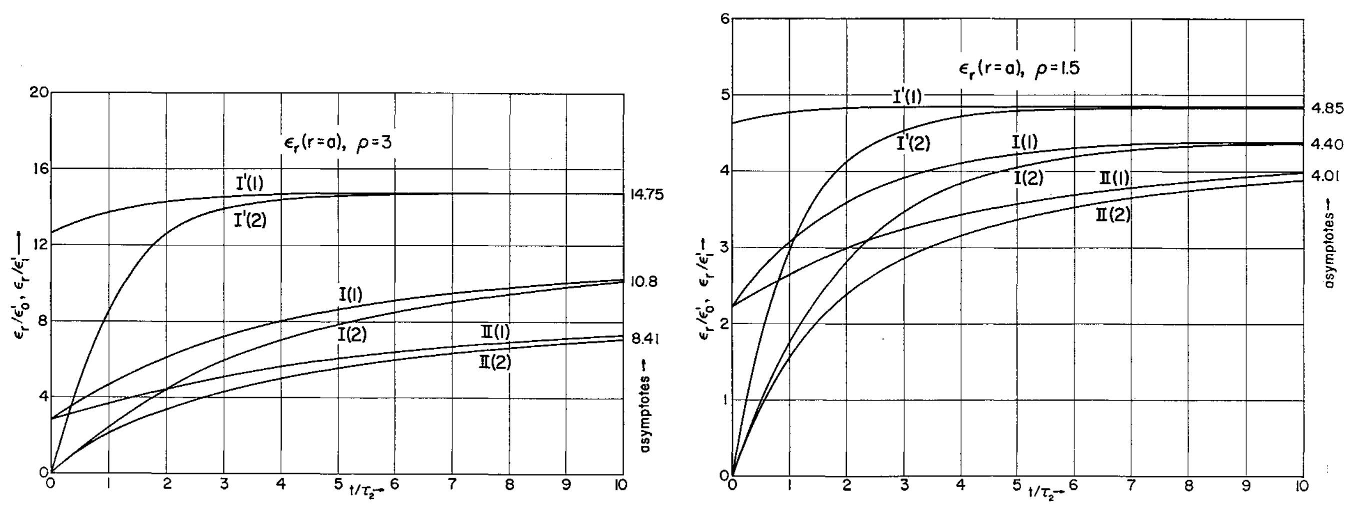

FIG. 5. Radial strain ϵ_r at $r = a$ as a function of time (t/τ_2).

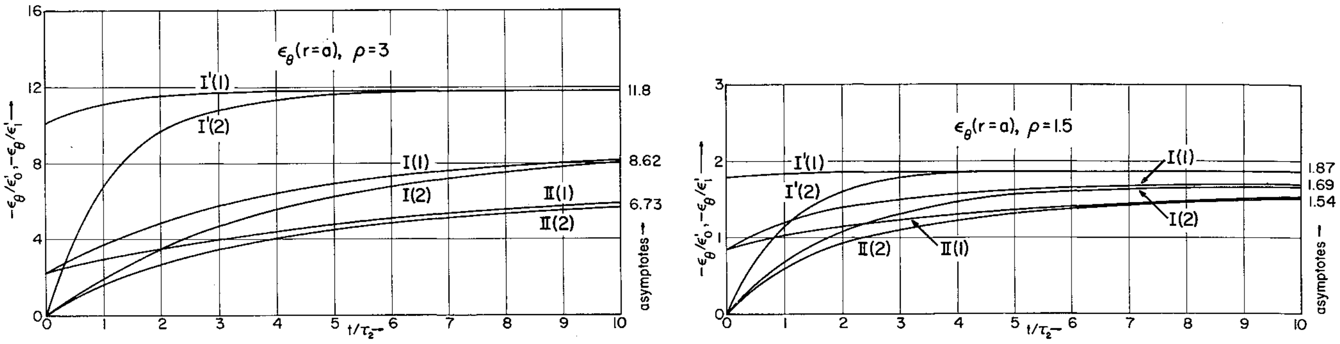

FIG. 6. Tangential strain ϵ_θ at $r = a$ as a function of time (t/τ_2).

$\bar{F}_\epsilon(p)$ in the previous section are simplified as follows.

(a) Model I

$\epsilon' = \epsilon_0' H(t)$

$$\bar{F}_\sigma(p) = \frac{\epsilon_0' K(Gp + G_1/\tau_2)}{p(p - k)} \tag{22}$$

$$\bar{F}_\epsilon(p) = \frac{\epsilon_0' K(p + 1/\tau_2)}{p(p - k)} \tag{23}$$

$\epsilon' = \epsilon_1'(1 - e^{-t/\tau_2})H(t)$

$$\bar{F}_\sigma(p) = \frac{\epsilon_1' K(Gp + G_1/\tau_2)}{\tau_2 p(p + 1/\tau_2)(p - k)} \tag{24}$$

$$\bar{F}_\epsilon(p) = \frac{\epsilon_1' K}{\tau_2 p(p - k)} \tag{25}$$

(b) Model II

For $G/K = 0.461538$, $G_1/G_2 = 0.1$, $K_1 = K_2 = K/2$, and $\tau_2' = \tau_2$, k_2 in Eq. (17) turns out to be $k_2 = -1/\tau_2$.

$\epsilon' = \epsilon_0' H(t)$

$$\bar{F}_\sigma(p) = \frac{\epsilon_0'(Gp + G_1/\tau_2)(Kp + K_1/\tau_2)}{p(p + 1/\tau_2)(p - k_1)} \tag{26}$$

$$\bar{F}_\epsilon(p) = \frac{\epsilon_0'(Kp + K_1/\tau_2)}{p(p - k)} \tag{27}$$

$\epsilon' = \epsilon_1'(1 - e^{-t/\tau_2})H(t)$

$$\bar{F}_\sigma(p) = \frac{\epsilon_1'(Gp + G_1/\tau_2)(Kp + K_1/\tau_2)}{\tau_2 p(p + 1/\tau_2)^2(p - k_1)} \tag{28}$$

$$\bar{F}_\epsilon(p) = \frac{\epsilon_1'(Kp + K_1/\tau_2)}{\tau_2 p(p + 1/\tau_2)(p - k_1)} \tag{29}$$

The computation has been performed for six combinations of three different materials and two assumptions concerning volumetric deformation as shown in Table 1. $\rho(= b/a)$ is taken $\rho = 3$ and 1.5.

It should be noted that the differences between *I* and *II* and between *I* and *I'* demonstrate, respectively, the effects of volume viscosity and of elastic compressibility of the viscoelastic material on the mechanical response to the imposed volume deformation.

Figs. 3 and 4 show the (absolute) maximum stresses (σ_r at $r = b$, σ_θ at $r = a$) as functions of time (t/τ_2) while the (absolute) maximum strains (ϵ_r, ϵ_θ at $r = a$) are plotted against time in Figs. 5 and 6. As typical space distributions of stress and strain, Fig. 7 shows σ_r, σ_θ, ϵ_r, and ϵ_θ in Model I with $\nu_0 = 0.3$ and $\rho = 3$ as functions of r.

Eq. (13) and Eq. (18) show that the sum of three normal components of stress tensor $J_1(= \sigma_{kk})$ which is probably responsible for cracking of the viscoelastic material is not a function of r but only of time t:

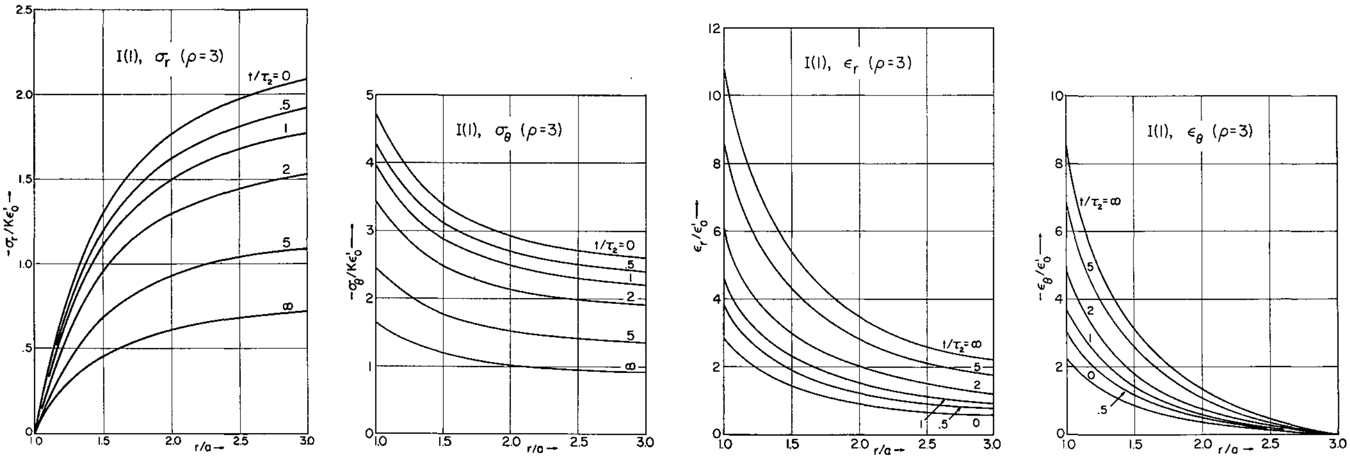

FIG. 7. Space distribution of stresses and strains.

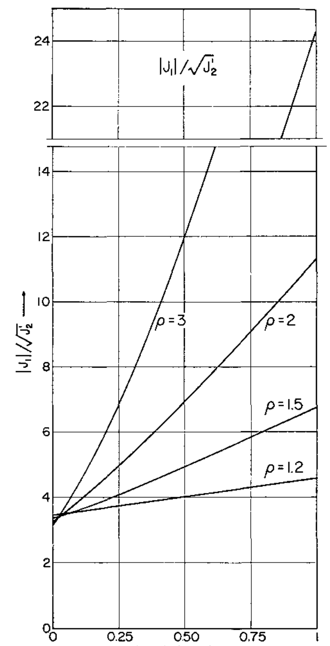

FIG. 8. Space distribution of $|J_1|/\sqrt{J_2'}$, the ratio of the first invariant of the stress tensor to the square root of the second invariant of the stress deviation tensor, as a measure of triaxiality of state of stress.

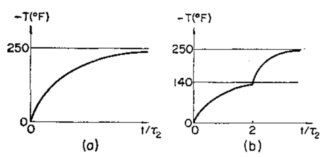

FIG. 9. Schematical illustration of temperature change in time (t/τ_2).

$$J_1 = -\frac{9(1 + 3\rho^2)}{3K + (1 + 3\rho^2)G} F_\sigma(t)$$

In order to investigate the degree of triaxiality of the stress, the ratio $J_1/\sqrt{J_2'}$ is computed and plotted as a function of space in Fig. 8, where J_2' is the second invariant of the stress deviation tensor.[1]

$$J_2' = \tfrac{1}{2}s_{ij}s_{ij} = \tfrac{1}{6}[(\sigma_r - \sigma_\theta)^2 + (\sigma_\theta - \sigma_z)^2 + (\sigma_z - \sigma_r)^2]$$

and therefore

$$J_1/\sqrt{J_2'} = -\sqrt{3}(1 + 3\rho^2)/\sqrt{1 + 3(\rho^2a^2/r^2)^2}$$

The last equation shows that the triaxiality ratio $J_1/\sqrt{J_2'}$ is independent of the type of model assumed.

Finally it is worth noting that $\sigma_z(t)$ is not a function of space but is identical with $\sigma_\theta(t)$ at $r = b$.

(6) Numerical Example (b)

The stresses and strains due to the following volumetric deformations are now considered.

$$\epsilon' = -1.375 \times 10^{-2} (1 - e^{-t/\tau_2}) H(t) \quad (30)$$

$$\epsilon' = -7.70 \times 10^{-3} (1 - e^{-t/\tau_2}) H(t) - 6.05 \times 10^{-3} [1 - e^{-(t/\tau_2 - 2)}] H(t - 2\tau_2) \quad (31)$$

The volumetric deformations in Eqs. (30) and (31) might be respectively associated with the temperature variation (Fig. 9a)

$$T = -250° (1 - e^{-t/\tau_2}) H(t)$$

and (Fig. 9b)

$$T = -140° (1 - e^{-t/\tau_2}) H(t) - 110° [1 - e^{-(t/\tau_2 - 2)}] H(t - 2\tau_2)$$

with an assumed coefficient of linear thermal expansion $\alpha = 5.5 \times 10^{-5}/°F$.

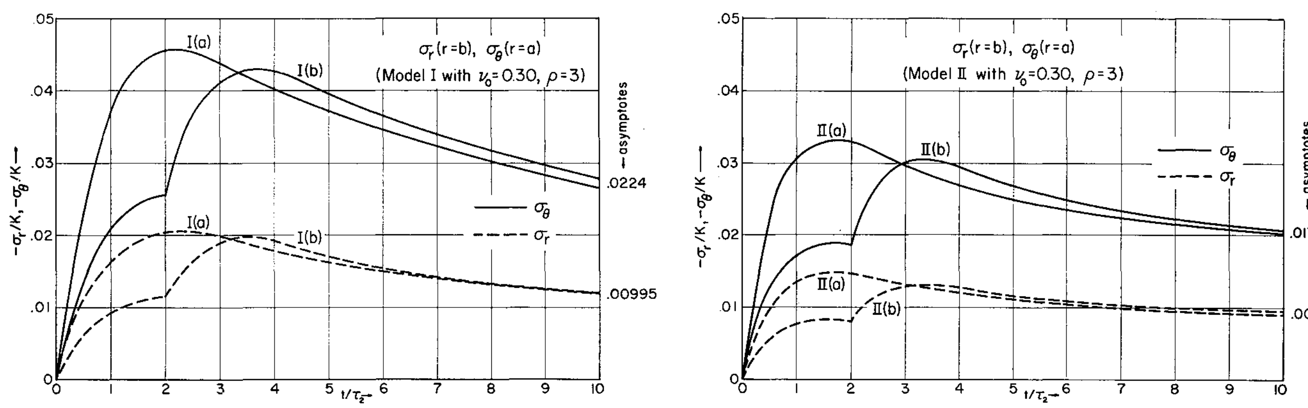

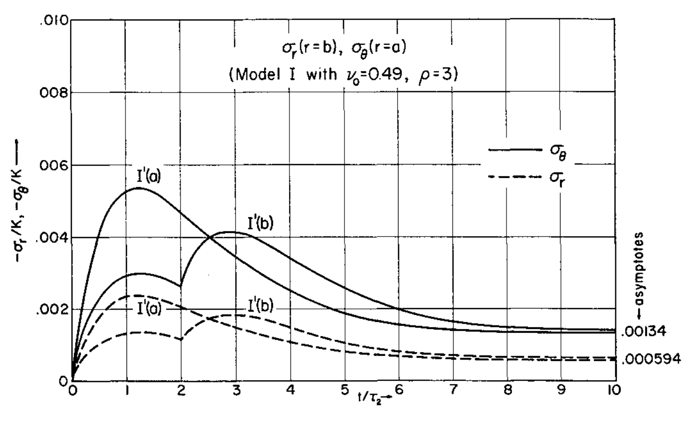

FIG. 10. Radial stress σ_r at $r = b$ and tangential stress σ_θ at $r = a$ caused by temperature change.

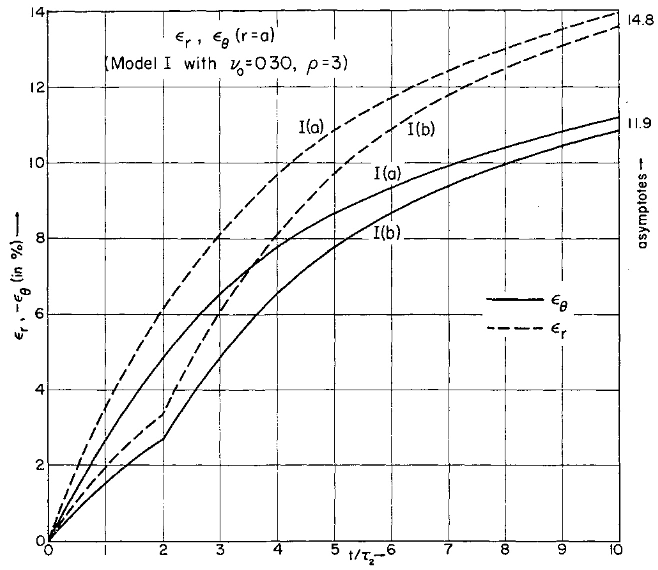

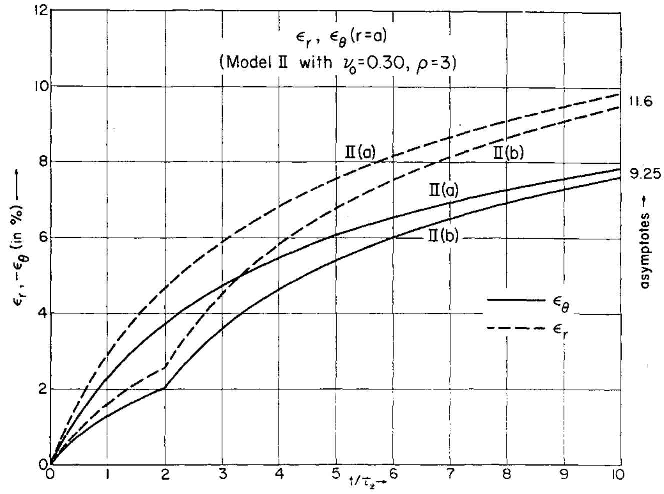

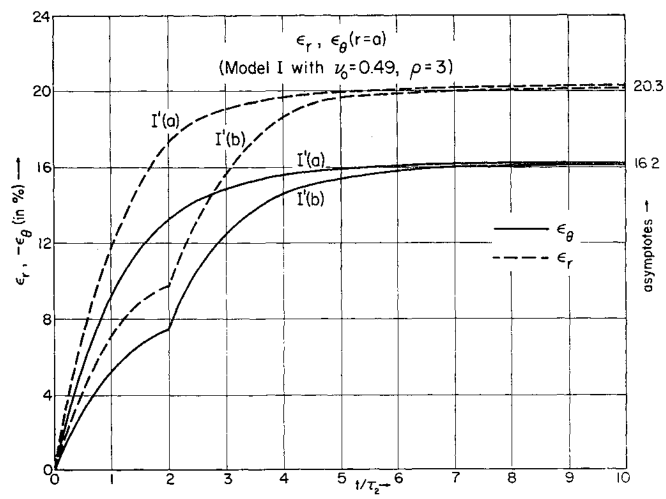

FIG. 11. Radial strain ϵ_r and tangential strain ϵ_θ at $r = a$ caused by temperature change.

The resulting stresses and strains due to these volume changes are of the form

$$\sigma_i(t) = -1.375 \times 10^{-2}\ \sigma_i^*(t)$$
$$\epsilon_i(t) = -1.375 \times 10^{-2}\ \epsilon_i^*(t)$$

for ϵ' given in Eq. (30) and

$$\sigma_i(t) = -7.70 \times 10^{-3}\ \sigma_i^*(t) - 6.05 \times 10^{-3}\ \epsilon_i^*(t - 2\tau_2)$$
$$\epsilon_i(t) = -7.70 \times 10^{-3}\ \epsilon_i^*(t) - 6.05 \times 10^{-3}\ \epsilon_i^*(t - 2\tau_2)$$

for ϵ' given in Eq. (31), where the suffix i stands for r, θ, and z and $\sigma_i^*(t)$ and $\epsilon_i^*(t)$ are the stress and strain response to the volume change $\epsilon' = +(1 - e^{-t/\tau_2})\ H(t)$ which can be easily obtained from the appropriate equations in the previous sections.

Dealing with the same models as discussed in Section 5, the computation has been performed for six combinations of three different materials and two assumptions concerning volume change as shown in Table 2. $\sigma_r(t)$ at $r = b$ and $\sigma_\theta(t)$ at $r = a$ for $\rho = 3$ are plotted in Figs. 10 and $\epsilon_r(t)$ and $\epsilon_\theta(t)$ at $r = a$ in Figs. 11.

With G at room temperature (rubber elastic state) of the order of magnitude of at least $G = 300$ psi, the order of magnitude of K is (a) for $\nu_0 = 0.3$, $K = 650$ psi and (b) for $\nu_0 = 0.49$, $K = 14{,}900$ psi. Hence the maximum radial stresses at the interface of grain and case and maximum tangential stresses at the inner surface are $\sigma_r = +13.7$ psi and $\sigma_\theta = +30.0$ psi for Model I with $\nu_0 = 0.3$, $\sigma_r = +9.75$ psi, and $\sigma_\theta = +21.6$ psi for Model II with $\nu_0 = 0.3$ and $\sigma_r = +35.8$ psi and $\sigma_\theta = +80.0$ psi for Model I with $\nu_0 = 0.49$, while the maximum strains at the inner surface are respectively $\epsilon_r = -0.148$ and $\epsilon_\theta = +0.119$, $\epsilon_r = -0.116$ and $\epsilon_\theta = +0.0925$, and $\epsilon_r = -0.203$ and $\epsilon_\theta = +0.162$.

With an increase of the shear modulus throughout

TABLE 2.

Model	ν_0	Volumetric Deformation ϵ'	Designation
I	0.3	Eq. (30)	I(a)
I	0.3	Eq. (31)	I(b)
II	0.3	Eq. (30)	II(a)
II	0.3	Eq. (31)	II(b)
I	0.49	Eq. (30)	I'(a)
I	0.49	Eq. (31)	I'(b)

the transitive range to at least 10^2 of the above values at the glass-transition temperature, the stresses in this range will also increase by a factor of at least 10^2 of the computed stresses.

Reference

[1] Freudenthal, A. M., and Geiringer, H. "The Mathematical Theories of the Inelastic Continuum," *Encyclopedia of Physics* (Handbuch der Physik), pp. 269–273, 293–296, 240; Springer-Verlag, Berlin, 1958.

✦ ✦ ✦

✦ ✦ ✦